

# Characterization of Porous Glasses by Adsorption: Models, Simulations and Data Inversion

Lev D. Gelb and K. E. Gubbins

North Carolina State University  
Department of Chemical Engineering  
Raleigh, NC 27695-7905, USA

Email: gelb@unity.ncsu.edu, keg@ncsu.edu

## Abstract

We have generated molecular models for adsorption in porous glasses that reproduce the complex structures of these materials, using simulations that mimic the quench processes by which Vycor and Controlled Pore Glasses are produced. We have simulated the adsorption and desorption isotherms for two of these model materials. In this work we compare pore size distributions calculated with the Barrett-Joyner-Halenda (BJH) method of isotherm analysis with geometrically-defined pore size distributions.

(translated abstract goes here)

## 1. Introduction

Controlled pore glass is widely used as a stationary phase in chromatography [1,2]. Controlled pore glasses (CPGs) and the related Vycor glasses have excellent mechanical properties and can be prepared with a wide range of porosities and pore sizes [3]. They can be modified to include a variety of functional groups, and the adsorption strength of the glasses can be adjusted over a wide range of values [2]. Although controlled pore glasses were developed for use in size-exclusion chromatography, derivatized glasses can show a high chemical affinity for certain biomolecules, and can even be used as catalytic agents and bioreactors [1].

The original preparations and characterizations of controlled pore glasses were done by Haller [4]. The starting material is 50–75%  $\text{SiO}_2$ , 1–10%  $\text{Na}_2\text{O}$ , and the remainder  $\text{B}_2\text{O}_3$ . The molten glass mixture is phase-separated by cooling to between 500 and 750 °C. The *time* taken for this treatment determines the extent of phase separation and the resulting average pore size. The borate phase is leached out by acid solutions at high temperatures. The remaining glass contains colloidal silica particles, which are removed by a treatment with NaOH followed by washing with water. The final glass has a porosity between 50% and 75%, and an average pore size between 4.5 nm and 400 nm. CPG has a surface area between 10 and 350  $\text{m}^2/\text{g}$ , depending on the pore size [2].

Vycor (or “thirsty”) glasses are prepared by a similar procedure [3]. Vycors have a porosity near 28%, an average internal pore diameter between 4 and 6 nanometers, and a surface area between 90 and 200  $\text{m}^2/\text{g}$  [3].

Porous glasses are usually characterized using standard nitrogen adsorption techniques. Although there has been considerable interest in the physics of flow, diffusion, and adsorption in these materials, there have been relatively few complete characterizations of porous glasses, and much of their structure is not very well understood.

## 2. Preparation of Glass Models

In a previous work [5] we have developed a procedure for the preparation of model glass structures, which mimics the preparation of experimental glasses. The resulting models have reasonable pore sizes, porosities and surface areas, show isotherms comparable with those measured by experiment, and are similar in appearance. A brief summary of this procedure is:

1. A large simulation cell containing a *symmetric* Lennard-Jones binary mixture is prepared, at a reduced density of  $\rho^* = 0.868$ . The inter-species well-depth, ( $\epsilon_{12}$ ) is set equal to  $0.25\epsilon_{11}$  in order to induce liquid-liquid immiscibility.
2. Using molecular dynamics simulation, this system is equilibrated at a (high) reduced temperature of  $T^* = 5.0$  for 4000 time steps of length  $0.005\tau$ . A Gaussian isokinetic thermostat and third-order Gear predictor-corrector integrator are used throughout.
3. The system is quenched to  $T^* = 0.75$  which induces phase separation. The trajectory is continued until the desired degree of separation is reached.
4. The final configuration from the quench run is quenched further to  $T^* = 0.01$  for an additional 1000 time steps, to relax the surface structure and solidify the material.
5. All atoms of species “2” are removed from the system. Uncoordinated molecules of component “1” are also removed.

For the study presented here, the simulation cell measured 27 nm on each side, and initially contained 868,000 particles. The initial mole fraction was  $X = 0.7$ . The quench simulations were run for 45,000 and 90,000 time steps, in order to produce finished models with average pore sizes near 3 nm and 5 nm, respectively.

A series of snapshots from the quench simulation is shown in Figure 1. At zero time, the two liquids are well-mixed. At later times the liquids separate in a complex way, forming *fully connected* networked structures which resemble cylinders at a very local scale, but which have many “defects” and intersections. The lower left and right configurations in this series were used to make the pore systems used in this study.

In order to simulate the adsorption of nitrogen in these model pores, we represent the nitrogen molecule with a single Lennard-Jones sphere, with potential parameters  $\sigma_N = 0.375$  nm and  $\epsilon_N/k_B = 95.2$  K [6]. The parameters for the substrate atoms are set to  $\sigma = 0.27$  nm and  $\epsilon/k_B = 230$  K, which have been used to represent bridging oxygens in silica [7]. The Lorentz-Berthelot mixing rules are used to give the inter-species parameters. All potential energy functions in the adsorption simulations were cut and shifted at  $r_c = 3.5\sigma$ ; no long-range corrections were used. Reference values for the saturation pressure were determined by Gibbs Ensemble Monte Carlo simulation, and the virial equation of state was used to convert between chemical potentials and pressures.

## 3. Geometric Characterization of Glass Models

As in our previous study of these materials [5] we have determined the porosity of the system by Monte Carlo volume integration [8]; the small-pore system was found to be  $28.9 \pm 0.1\%$  porous, and the large-pore system  $31.1 \pm 0.1\%$  porous.

We have also determined the surface area of both of these samples using the BET [9] isotherm method; a reference monolayer density for this analysis was taken from similar simulations on an amorphous planar surface [5]. The surface areas were found to be  $138 \pm 1$  m<sup>2</sup>/g for the small-pore system and  $82.9 \pm 0.6$  m<sup>2</sup>/g for the large-pore system.

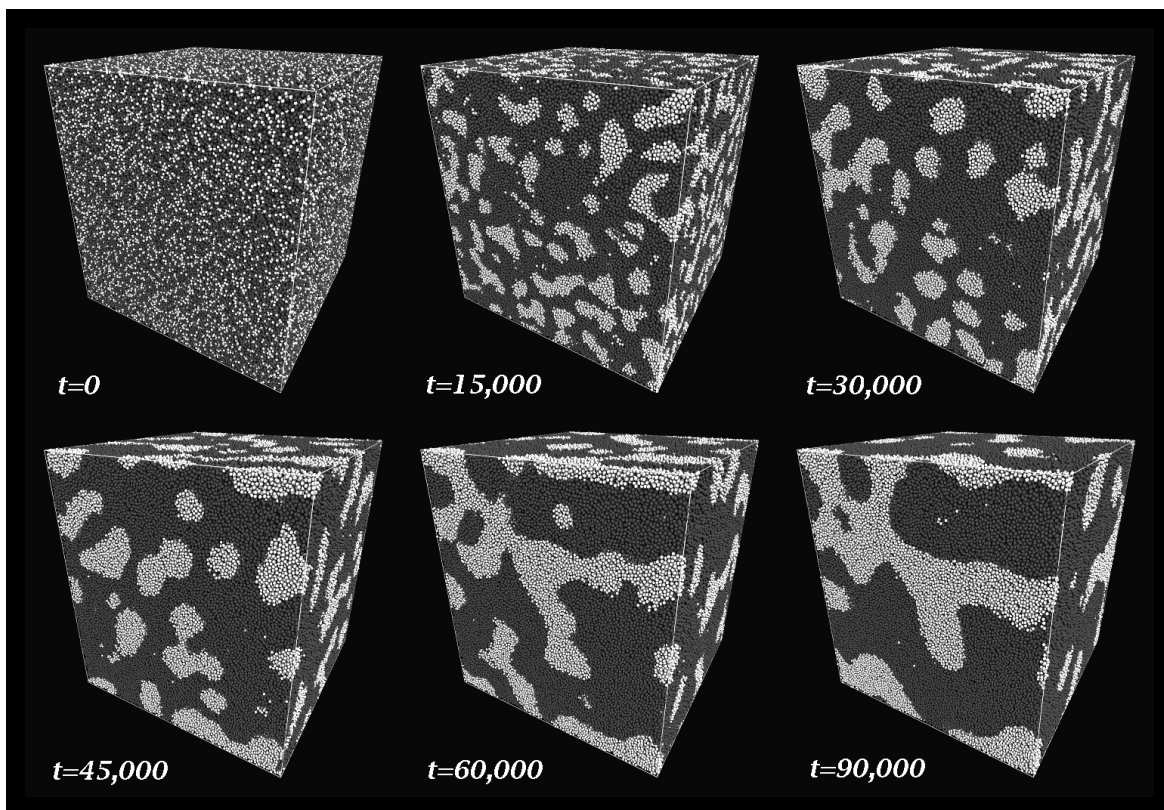


**Figure 1.** Snapshots from the quench run. Pictures are taken at times of 0 (at the quench), 15,000 steps, 30,000 steps, 45,000 steps, 60,000 steps and 90,000 steps. The darker phase will become the porous substrate in later simulations, and the volume occupied by the lighter phase will become the void.

The geometric definitions of surface area and porosity are intuitive. With a little added complexity, we can also define a geometrical pore size distribution. Consider the sub-volumes of the system accessible to spheres of different radii. Let  $V_{\text{pore}}(r)$  be the volume of the void space “coverable” by spheres of radius  $r$  or smaller; it is easy to see that  $V_{\text{pore}}(r)$  is a monotonically decreasing function of  $r$ . This function is easily compared with the “cumulative pore volume” curves often calculated in isotherm-based PSD methods. The derivative  $-dV_{\text{pore}}(r)/dr$  is the fraction of volume coverable by spheres of radius  $r$  but *not* by spheres of radius  $r + dr$ . When normalized, this function *is* a geometric definition of the pore size distribution [10]. The  $V_{\text{pore}}(r)$  function can be calculated by a Monte Carlo procedure in which randomly chosen points are tested to see if they are covered by a sphere of radius  $r$  that itself does not overlap with any substrate atoms.

For the specific case of a material composed only of straight cylinders, the PSDs calculated in this fashion and those inferred by the BJH method of isotherm analysis (see below) should be identical. For a material composed of spherical pores, this analysis would give the exact distribution of sphere sizes. For a material with irregularly shaped pores, this geometric pore size definition is still fully applicable, while the assumptions that underly many isotherm-based analysis methods may not apply.

#### 4. Calculation of Adsorption Isotherms

Grand Canonical Monte Carlo is a stochastic scheme which simulates an *open* system with fixed temperature, chemical potential, and volume. It is the appropriate method to use for determining adsorption isotherms by computer simulation. The specific details and mathematics of this scheme can be found elsewhere [11]. Due to the extremely large size of the simulation cells used in this study, we have used a version of the GCMC algorithm recently developed for

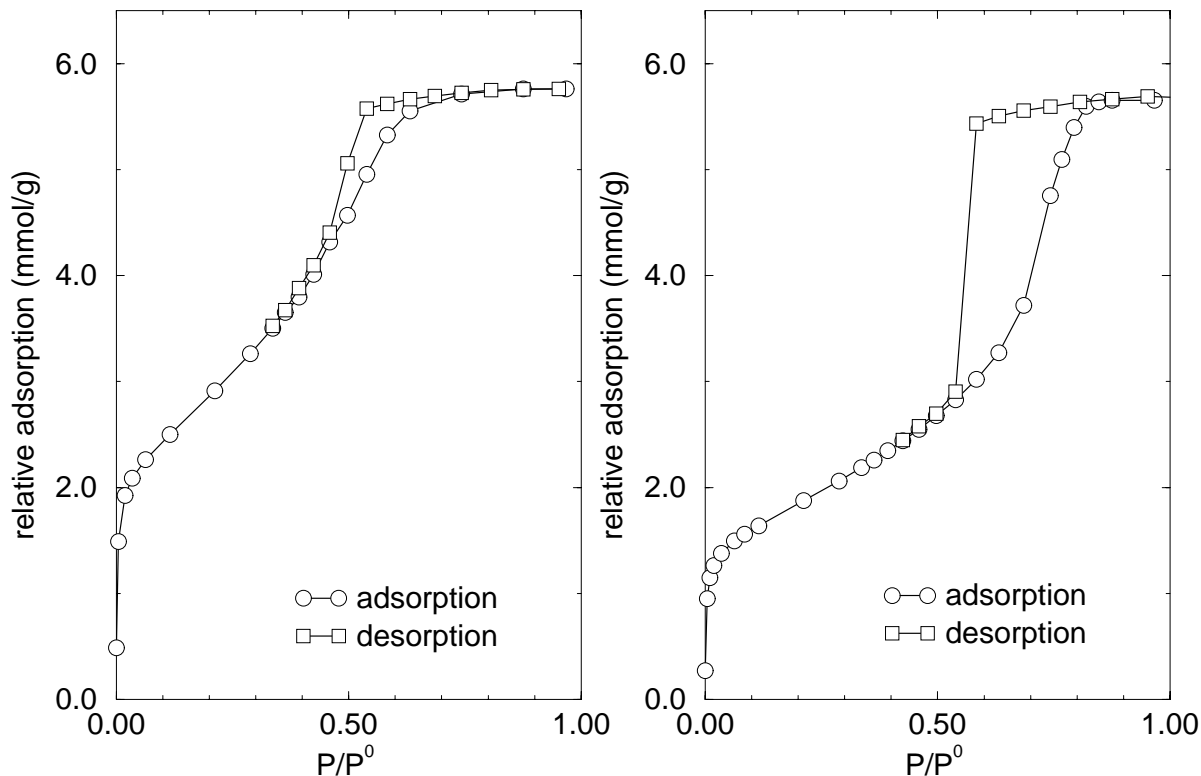


**Figure 2.** Adsorption and desorption isotherms, in the small-pore (left) and large-pore (right) systems. Adsorption excess is given in units of mmol adsorbate per gram adsorbent, plotted against relative pressure. The adsorption branch points are shown as circles, and desorption data as squares. Errors are smaller than the symbols used.

parallel computers [12].

For the simulations at low relative pressures all calculations were run for 60 million equilibration moves, followed by 60 million moves for data collection. For higher pressures, we found that 100 million moves were necessary to equilibrate the system.

The adsorption and desorption isotherms in both systems are shown in Figure 2. In both cases, the adsorption branch of the data is extremely smooth. Both systems show hysteresis in the isotherms, clearly indicating a first-order capillary condensation transition.

We note that in Monte Carlo simulations of adsorption, hysteresis is due to the presence of thermodynamically metastable states in the system and *not* to kinetic effects such as “pore-blocking.” This affects both the shape and interpretation of these isotherms; many methods for calculating PSDs from desorption isotherms cannot be applied here, since the mechanisms of pore emptying are different in simulation and experiment. In this study we only apply isotherm-based analysis methods to the *adsorption* branch of the isotherm.

## 5. Pore Size Distribution Analyses

The Barrett-Joyner-Halenda (BJH) method for calculating pore size distributions [13] is based on a model of the adsorbent as a collection of cylindrical pores. The theory accounts for capillary condensation in the pores using the classical Kelvin equation, which in turn assumes a hemispherical liquid-vapor meniscus and a well-defined surface tension. The BJH theory also incorporates thinning of the adsorbed layer through the use of a reference isotherm; the Kelvin equation is only applied to the “core” fluid.

In the original BJH formulation, a simplifying approximation is introduced in which the  $c$  parameter, which is essentially the ratio of core radius to pore radius, is assumed constant. In our calculations this assumption is relaxed and the “full” BJH theory is used; this is our only deviation from the original approach [13].

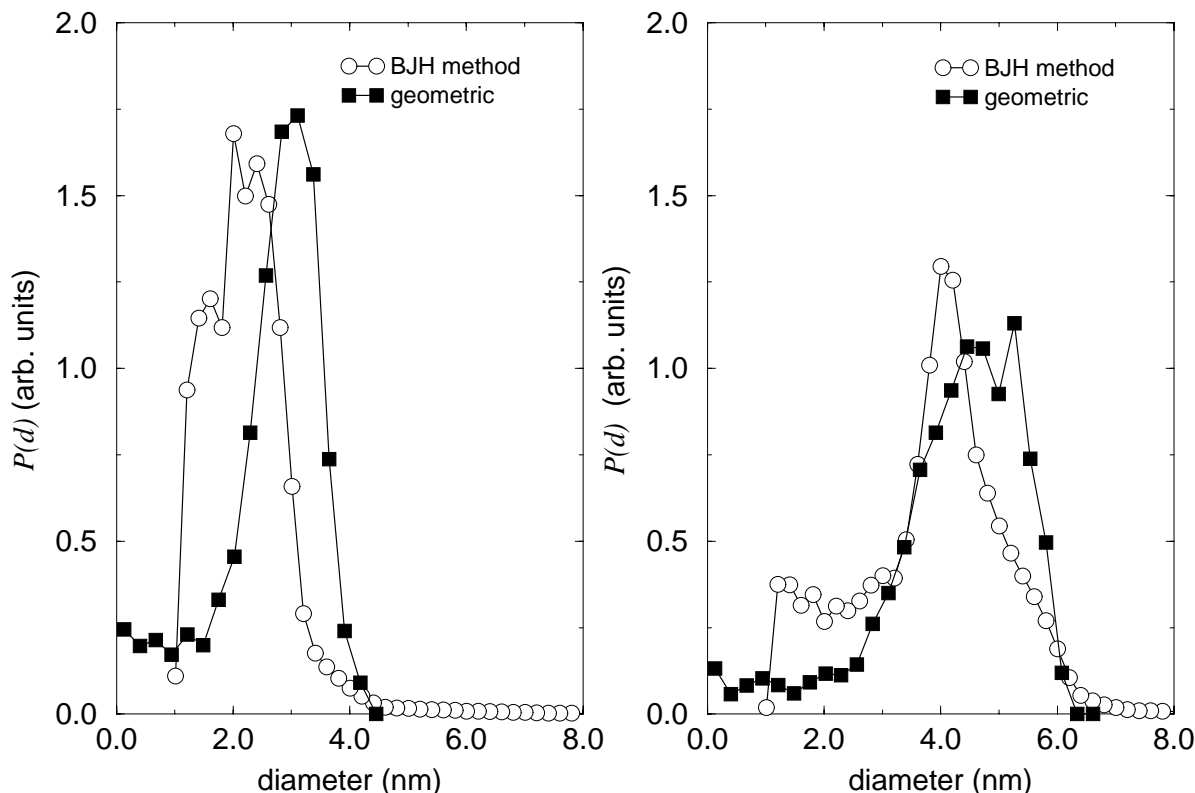


**Figure 3.** Comparison of pore size distributions, in the small-pore (left) and large-pore (right) systems. Data obtained by BJH analysis of adsorption isotherms are compared with a geometrically-defined quantity.

We have measured a reference isotherm by simulation of adsorption on an amorphous planar system with potential parameters identical with those in the glass system. These data were fitted with a modified BET isotherm [14], and the analytical fit was used as input to the BJH calculation. The value of the surface tension used was interpolated from previous simulations of the Lennard-Jones liquid [15, 16].

In Figure 3 are the pore size distribution curves for both systems, from both the BJH analysis of adsorption isotherm data and the geometric definition. In the small-pore system, the geometric data are slightly narrower, and the BJH data are shifted to a smaller pore diameter. The BJH data also show a weak tail at large pore diameters, which is not found in the geometric PSD data. In the large-pore system, the agreement between peak locations is better (though still not very good), but the shape of the two curves is somewhat different. The BJH data show a long tail at large pore diameters not found in the geometric data, and also have larger values at most small pore diameters.

In both cases, the likely cause of the discrepancy between geometric and isotherm-derived PSD peak positions is the application of the Kelvin equation to these systems. It is well-known [17] that the surface tension of a very small meniscus increases with decreasing capillary radius. Increasing the surface tension has the effect of scaling the pore size distribution to larger diameters; therefore, using a bulk value of the surface tension leads to an underestimation of the average pore size. We have found that if we arbitrarily adjust the surface tension upwards by about 25%, the peak locations in both systems are brought into agreement.

However, this correction causes a further difficulty. If the BJH curve is so scaled, then the large-diameter tail of the distribution extends significantly further than that of the geometric distribution; e.g., the BJH model predicts the presence of pores considerably larger than the largest spherical void space found anywhere in the material. This may be due to the use of the adsorption isotherm in the BJH analysis. The long tail could be caused by the (metastable) part of the adsorption isotherm at high pressures, where the pores *should* be filled with liquid, but

are not. Since the thermodynamic transition between liquid-like and vapor-like states occurs at pressures below the top of the hysteresis loop, we expect that use of only the adsorption data would lead to artificially high pore sizes.

Lastly, we point out that the relative differences in peak position are greater in the small-pore system than in the large-pore system. This supports the general assumption that Kelvin equation-based analysis methods are less reliable for small pores than for large pores. Our BJH data show significant deviations from geometrically-defined properties even for the large-pore system, suggesting that 5 nm porous glasses (such as Vycor) are too small to be reliably characterized using this technique.

We thank the National Science Foundation (grant no. CTS-9508680) for their support of this work and for a Metacenter grant (no. MCA93S011P) which made these calculations possible, and the staffs of the Cornell Theory Center and Pittsburgh Supercomputing Center for their general assistance.

## References

- [1] W. Haller, Application of controlled pore glass in solid phase biochemistry, in: W. H. Scouten (ed.), *Solid Phase Biochemistry*, John Wiley and Sons, New York, 1983 535–597.
- [2] R. Schnabel, P. Langer, Controlled-pore glass as a stationary phase in chromatography, *J. Chromatography* (1991), 544, 137–146.
- [3] T. H. Elmer, Porous and reconstructed glasses, in: S. J. Schnieder, Jr. (ed.), *ASM Engineered Materials Handbook*, vol. 4, ASM, Materials Park, OH, 1991 427–432.
- [4] W. Haller, Chromatography on glass of controlled pore size, *Nature* (1965), 206, 693–696.
- [5] L. D. Gelb, K. E. Gubbins, Characterization of porous glasses: Simulation models, adsorption isotherms, and the BET analysis method, *Langmuir* (1998), in press.
- [6] M. W. Maddox, J. P. Olivier, K. E. Gubbins, Characterization of MCM-41 using molecular simulation: heterogeneity effects, *Langmuir* (1997), 13, 1737–1745.
- [7] A. Brodka, T. W. Zerda, Properties of liquid acetone in silica pores: Molecular dynamics simulation, *J. Chem. Phys.* (1996), 104, 6319–6326.
- [8] E. E. Underwood, *Quantitative Stereology*, Addison-Wesley, Reading, MA (1970).
- [9] S. Brunauer, P. H. Emmett, E. Teller, Adsorption of gases in multimolecular layers, *J. Amer. Chem. Soc.* (1938), 60, 309.
- [10] P. Pfeifer, G. P. Johnston, R. Deshpande, D. M. Smith, A. J. Hurd, Structure analysis of porous solids from preadsorbed films, *Langmuir* (1991), 7, 2833–2843.
- [11] M. P. Allen, D. J. Tildesley, *Computer simulation of liquids*, Clarendon Press, Oxford (1987).
- [12] G. S. Heffelfinger, M. E. Lewitt, A comparison between two massively parallel algorithms for Monte Carlo computer simulation: An investigation in the grand canonical ensemble, *J. Computat. Chem.* (1996), 17, 250–265.
- [13] E. P. Barrett, L. G. Joyner, P. P. Halenda, The determination of pore volume and area distributions in porous substances. I. Computations from nitrogen isotherms, *J. Am. Chem. Soc.* (1951), 73, 373–380.
- [14] S. Brunauer, J. Skalny, E. E. Bodor, Adsorption on nonporous solids, *J. Coll. Int. Sci.* (1969), 30, 546–552.
- [15] C. D. Holcomb, P. Clancy, J. A. Zollweg, A critical study of the simulation of the liquid-vapour interface of a Lennard-Jones fluid, *Mol. Phys.* (1993), 78, 437–459.
- [16] G. A. Chapela, G. Saville, S. M. Thompson, J. S. Rowlinson, Computer simulation of a gas-liquid surface part 1., *J. Chem. Soc. Faraday Trans. II* (1977), 73, 1133–1144.
- [17] R. C. Tolman, The effect of droplet size on surface tension, *J. Chem. Phys.* (1949), 17, 333–337.